Development of a Poundo-yam Single Screw Extruder

Olorunsogo, Samuel Tunde; Awonorin, Samuel Olusegun

Abstract— Poundo-yam is a very popular food product in the yam production zone of West Africa. However, the traditional process for making poundo-yam is tedious, laborious, energy demanding, time consuming, and the pounding generates a large volume of sweat, not all of which escapes the food. In this research work a low speed single screw poundo-yam extruder was designed, fabricated using locally available materials and its performance evaluated.

Index Terms— Poundo-yam, Single Screw, Extruder, Feeding/conveying section, Transition/kneading section, Metering/mixing/texturizing section, Thrust Bearing, Speed reducing gear.

1 INTRODUCTION

Yams are processed into various food forms, which include poundo-yam (from *D. rotundata* and sometimes *D. cayenensis*), boiled yam, roasted or grilled yam, fried yam slices and yam balls, mashed yam, yam chips and flakes; but the greater part of the world's yam crop is consumed as poundo-yam. 'Poundo – yam' is a smooth dough made by peeling, boiling, pounding and kneading yam tubers. It is a very popular food product in the yam production zone of West Africa. In the middle belt, eastern and southern Nigeria, Ghana, Ivory Cost (Côte d'Ivoire), Benin and some other parts of West Africa, poundo-yam is classified as a special delicacy and a highly prestigious meal all over Africa. However, the traditional process for making poundo-yam is tedious, laborious, energy demanding, time consuming, and the pounding generates a large volume of sweat, not all of which escapes the food ([4] www.africanfoods.co.uk/yam.html).

Commercial preparation of poundo-yam based on scientific principles is still a challenging task, which has received, surprisingly, little attention in the literature. However, there are a couple of devices currently in use. The prominent of such devices is an automated yam blender ([1] www.idrc.org.sg). However, this device is very limited in capacity, basically batch system and could not give the characteristic texture and firmness found in traditionally prepared poundo-yam. Extrusion technology can be employed to solve the tedious, energy demanding, and time consuming yam pounding processing.

Extrusion is predominantly a continuous thermo-mechanical processing operation that combines several unit operations, including conveying, compressing, kneading, reacting, mixing, texturizing, shearing, shaping, and forming, depending on the material being processed and the equipment used (Mian, 2000).

- *Olorunsogo, S.T. is currently pursuing Ph.D degree Program in Food engineering from Department of Food Science and Technology, Federal University of Agriculture, Abeokuta, Nigeria. E-mail: olorunsogosam@yahoo..com, olorunsogosam@gmail..com.*
- *Awonorin, S.O. is a Professor of Food Engineering, Department of Food Science and Technology, Federal University of Agriculture, Abeokuta, Nigeria.*

2 MATERIALS AND METHODS

2.1 Design and Construction of Poundo-yam Extruder

The poundo-yam extruder comprises a barrel within which a graduating screw is rotatably mounted. The screw conveys material by viscous drag against the barrel. This resistance to forward movement causes the transported material to slip against itself, thus transforming mechanical energy into heat.

The barrel is divided in three functional longitudinal sections:

(a) feeding/conveying section,
(b) transition/kneading section, and finally a
(c) metering/mixing/texturizing section.

Screw output capacity was obtained by:

$$\dot{m} = cD_b^2 NH_m G \ (\text{Ibs/hr}) \qquad (1)$$

where, c = drag flow constant for 25:1 L/D screw (= 2.3)

$\dot{m}$ = mass flow rate in Ibs/hr

D_b = inside diameter of an extruder barrel (in inches)

N = screw speed (assume 15 rpm)

H_m = channel depth of metering=2.72mm (= 0.107in)

G = specific gravity of yam tuber ≅ 0.96 at extrusion temperature

Alternatively, the mass flow rate can be obtained by:

$$\dot{m} = D_b^2 \cdot N \cdot H_f \cdot \rho_{bulk} \qquad (2)$$

where, H_f = Feed channel depth in inches

N = Screw speed in revolutions per minute

θ = Helix angle

ρ_{bulk} = Bulk density in pounds per cubic inch.

The volumetric flow rate is given by ([2, 3] Anil Kumar et al., 1997; Chang, 2007):

$$\dot{v} = v_z \times W \times H_f \qquad (3)$$

where, $\dot{v}$ = volumetric flow rate $\left(in^3 / \min\right)$

v_z = Channel velocity = $\pi DN \cos\theta$

W = Feed channel width in inches

The screw diameter at the tip of the flights was given by ([4] Zehev et al., 2006):

$$D_{S_{Tip}} = D_b - 2\delta_f \qquad (4)$$.

where,

δ_f = a small radial clearance of the order of0.1- 0.3% of D_b.

Assuming a screw axial length L to diameter D (L/D) ratio of 25 : 1, the effective axial length of the screw was obtained by:

$$L = 25 \times D_b \qquad (5)$$

The length of feed/solid conveying section is 20.63% of screw length i.e. $\approx 0.2 \times L$. Length of the transition section is 47.94% of screw length i.e. $\approx 0.48 \times L$. Length of the metering section is 31.43% of screw length i.e. $\approx 0.31 \times L$.

The helix angle at the barrel surface, θ, which is related to lead and diameter is given by ([10] Zehev et al., 2006):

$$\tan\theta = \frac{L_s}{\pi D_s} \qquad (6)$$

The screw lead, L_s, becomes:

$$L_s = \pi D_{s_{Root}} \tan\theta \qquad (7)$$

The Channel width at the barrel surface is given by:

$$W = L_S \cos\theta - e \qquad (8)$$

where, e is the flight width.

The diameter of the screw at the root of the screw was given by:

$$D_{s_{Root}} = D_b - 2H_m \qquad (9)$$

In the feed/solid conveying and metering sections both H and D_s are constant, whereas, in the transition section they vary with axial position. In the metering section of an extruder, there is an optimum channel depth for maximum output or pressure.

2.1.1 The Deep Uniform-Channel Feeding/Solid Conveying Section Design

.The length of the feeding section is 31.43% of screw axial length L. i.e., $L_f = 0.2 \times L$. For effective compression at the downstream end of the barrel, the channel depths ratio $H_f : H_m$ is assumed to be 10:1. Thus,

$$H_f = 10 \times H_m \qquad (10)$$

The screw lead at the feeding section, from eqn. (7), was:

$$L_f^{'} = \pi D_{s_{Root}} \tan\theta \qquad (11)$$

The flight width is still assumed as 10% of diameter of the root of the screw at the feeding section, i.e., $\varepsilon = 0.1 \times D_{s_{Root}}$.

Channel width at the barrel surface in the feeding section,

$$W_f = L_f^{'} \cos\theta_b - \varepsilon \qquad (12)$$

The conveying mechanism in screw extruders is one of drag-induced flow. Using the drag flow term, volumetric drag flow rate in the screw extruder is:

$$Q_d = 0.5\pi ND_b WH \cos\theta_b \qquad (12)$$

At steady state, the yam tubers have a constant axial velocity $V_{ax.}$ and constant angular velocity V_θ. The axial velocity $V_{ax.}$ is related to the mass flow rate by:

$$\left.\begin{aligned} \dot{m}_s &= \rho_b HpWv_{ax} \\ &\text{or} \\ \dot{m} &= V_{ax.}\rho_{b_y}\left[\frac{\pi}{4}\left(D_b^2 - D_{s_{Root}}^2\right) - \frac{\varepsilon H_f}{\sin\theta}\right] \end{aligned}\right\} \qquad (13)$$

where, $\dot{m}_s$ = Conveying rate of the tuber slices

ρ_b = Solids bed density

H = Channel depth

p = number of parallel flights

W = Channel width

v_{sz} = Solid bed velocity in z-direction

ρ_{b_y} = bulk density of the feed.

The tangential velocity of the barrel surface,

$$V_b = \pi ND_b \qquad (14)$$

The angle of movement of the outer surface of the solid plug, ϕ, was obtained from:

$$V_{ax} = V_b \frac{\tan\phi \tan\theta_b}{\tan\phi + \tan\theta_b} \qquad (15)$$

The volumetric flow rate, Q_s, of the solid plug is the product of the axial component of the plug velocity and the area for flow in that direction,

$$Q_s = V_{ax}\pi DH \qquad (16)$$

which, in combination with Eq. (13), gives

$$Q_s = \left(\pi^2 D_b^2 NH\right)\left[\frac{\tan\phi \tan\theta}{\tan\phi + \tan\theta}\right] \qquad (17)$$

where all the quantities except ϕ are known.

As yam tubers (freely deformable solids) move down the channel, frictional forces are generated and results in a pressure rise in the feed section. This pressure compresses the solids bed into a plug which continues to travel down the channel. The pressure build-up is expressed in the general form ([2, 3] Anil Kumar et al., 1997; Chang, 2007):

$$\left.\begin{aligned} P &= P_o \exp\left(const \cdot f_b - const \cdot f_s\right) Z_b \\ P_0 &= \frac{\rho_b g D}{4 f_w' k} \end{aligned}\right\} \qquad (18)$$

where: P_0 = Pressure under the hopper (usually very small)

f_b, f_s = Friction coefficients of the solid bed on the barrel and screw (For forward motion f_b must be larger than f_s).

Z_b = Down channel distance

ρ_b = Material bulk density,

$g = 9.81\ \mathrm{m/s^2}$

k = Ratio of compressive stress in the horizontal direction to compressive stress in the vertical direction

D = Hopper neck diameter

Due to conical section used in the design, the pressure at the discharge opening into the solids conveying zone P_1 (the initial pressure in the solids conveying zone) cannot be equal to the pressure under the solids in the hopper, P_0. A rough estimate used was:

$$P_1 = f_w' P_0 = 0.3 P_0 \qquad (19)$$

where,

f_w' = The static frictional coefficient between yam tubers and the hopper wall

The pressure rise in the solids conveying region is given by ([2, 3] Anil Kumar et al., 1997; Chang, 2007):

$$p = p_B \exp\left(-\frac{\left(A_1 K - B_1\right)}{\left(A_2 K + B_2\right)} z\right) \qquad (20)$$

where, $A_1 = f_b W \sin\phi + 2 H f_s \sin\theta + W f_s \sin\theta$

$$A_2 = HW \sin\theta$$

$$B_1 = f_b W \cos\phi - 2 H f_s \cos\theta - W f_s \cos\theta$$

$$B_2 = HW \cos\theta$$

$$K = \frac{\bar{D}}{D_b} \frac{\sin\bar{\theta} + f_s \cos\bar{\theta}}{\cos\bar{\theta} - f_s \sin\bar{\theta}}$$

$$\bar{D} = 1/2\left(D_b + D_{s_{Root}}\right)$$

$\bar{\theta}$ = mean helix angle

The ratio pressure at any down-channel distance $Z_b \left(= D_b/\theta\right)$ of the solids conveying to the initial pressure at $z_b = 0$, i.e. P_2/P_1 was obtained from ([2, 3] Anil Kumar et al.,1997; Chang, 2007):

$$\left.\begin{aligned} M = 2\frac{H}{W_b}\frac{f_s}{f_b}\sin\theta_b\left(K + \frac{\bar{D}}{D_b}\cot\bar{\theta}\right) + \frac{W_s}{W_b}\frac{f_s}{f_b}\sin\theta_b\left(K + \frac{D_s}{D_b}\cot\theta_s\right) \\ + \frac{\bar{W}}{W_b}\frac{H}{Z_b}\frac{1}{f_b}\sin\bar{\theta}\left(K + \frac{\bar{D}}{D_b}\cot\bar{\theta}\right)\ln\frac{P_2}{P_1} \end{aligned}\right\} (21)$$

where,

$\bar{\theta}$ = Mean helix angle

$\bar{W}$ = Mean channel width

$\bar{D} = 1/2\left(D_b + D_{s_{Root}}\right)$

M was obtained from the expression:

$$\cos\phi = K_s \sin\phi + M \qquad (22)$$

Frictional forces lead to surface-heat generation. The total power introduced through the shaft is partly dissipated into heat at the barrel, flights, and root of the screw surfaces, and is partly used to generate pressure. However, most of the power is dissipated into heat at the barrel surface. ([3] Chang, 2007). The heat q_b generated by friction on the barrel surface along the screw axis z is related to the pressure p by ([3] Chang, 2007):

$$q_b = p f_b W V_b \left(\frac{\sin\theta}{\sin\left(\theta + \phi\right)}\right) \qquad (23)$$

where, W is the channel width, f_b is the friction coefficient, V_b is the barrel velocity, θ is the flight helix angle, and ϕ is the angle of movement of the outer surface of the solid plug.

The total power consumption in the solids conveying zone was obtained by ([10] Zehev et al., 2006):

$$P_w = \pi N D_b W_b Z_b f_b \cos\phi \frac{P_2 - P_1}{\ln\left(P_2/P_1\right)} \qquad (24)$$

where, P_1 is the initial pressure at $z = 0$ and P_2 is the pressure at any down-channel distance z_b, where, solids conveying is the only elementary step taking place.

Clearly, once the tubers start melting, the frictional drag conveying mechanism changes into a viscous drag mechanism

(Chang, 2007). The heat generated at the barrel surface, given by Eq. (23), is dissipated into the solid plug and conducted away through the barrel walls.

2.1.2 The Tapered Transition/Kneading Section Design

In the transition section both H_t and D_s vary with axial position. Within this section the channel depth becomes shallower and pressure profile exhibits a maximum in this tapered section. The mechanism of shear begins to play a dominant role. Density increases and the extrudate begins to lose some of its solid definition. The crushed tubers received from the feeding/solid conveying section are compressed, melted and transported. The compressive action causes more frictional heat which causes the yam slices to melt. The homogeneous mass are further melted and properly mixed.

To achieve both good conveying and good kneading, a helix angle in the range of $\theta = 25^0$ was used.

Length of the transition section is 47.94% of screw length.

i.e., $L_t = 47.94\% \times 1648mm = 790mm$

In the transition section both H_t and $D_{s_{Root}}$ vary with axial position:

$$2.7mm \le H_t \le 27mm \text{ and } 11mm \le D_{s_{Root}} \le 60mm.$$

Thus, the screw lead in the transition section is obtained from eqn. (7)

i.e. $L_t^{'} = \pi D_{s_{Root}} \tan\theta.$

The flight width is still assumed as 10% of diameter of the root of the screw

i.e., $\varepsilon = 0.1 \times D_{s_{Root}}$.

Channel width at the barrel surface,

$$W_t = L_t^{'} \cos\theta_b - \varepsilon \qquad (25)$$

Helix angle at the root of the screw,

$$\theta_s = \theta_b + \psi, \quad 2.5 \le \psi \le 3.0. \qquad (26)$$

Mean helix angle,

$$\overline{\theta} = (\theta_b + \theta_s)/2 \qquad (27)$$

The axial velocity $V_{ax.}$ in the transition section is obtained from eqn. (13)

To calculate the pressure at the end of the transition section, P_3, the constants K_s and M were obtained from appropriate equations (20), (21), and (22).

The power introduced through the shaft at the transition section was obtained from Equation (24).

2.1.3 The Shallow Metering Section Design

The shallow metering section gives the dough uniform pressure and flow characteristics. The dough is texturized, plasticized, blended, kneaded, and pushed against the downstream side plate (the breaker plate).

To achieve a good conveying, texturization, plasticization, blending, and kneading, a helix angle at the barrel surface, $\theta_b = 27^0$, was chosen. Length of the metering section is 31.43% of screw axial length L. i.e., $L_m = 0.3143 \times L$

In the metering section both H and D_s are constant.

In the metering section, the diameter of the screw at the root of the screw was given by:

$$D_{s_{Root}} = D_b - 2H_m \qquad (28)$$

The screw lead, from eqn. (7),

$$L_m^{'} = \pi D_{s_{Root}} \tan\theta \qquad (29)$$

The flight width is still assumed as 10% of diameter of the root of the screw i.e., $\varepsilon = 0.1 \times D_{s_{Root}}$.

Channel width at the barrel surface,

$$W_m = L_m^{'} \cos\theta_b - \varepsilon \qquad (30)$$

In the metering section of an extruder, there is an optimum channel depth for maximum output or pressure. The optimum channel depth, H_{op} was obtained by (Zehev et al., 2006) :

$$H_{op} = \frac{3Q}{\pi NWD_b \cos\theta_b} \qquad (31)$$

where, $Q =$ Volumetric flow rate.

The tangential velocity of the barrel surface, V_b, the angle of movement of the outer surface of the plug, ϕ, and the axial velocity $V_{ax.}$ of the extrudate along the barrel at the metering section wereestimated using Equations (14), (15), and (16), respectively. The volumetric flow rate in the screw extruder remains the same. To calculate the pressure at the end of the metering section, P_4, the constants K_s and M were obtained from appropriate equations (20), (21), and (22). The power introduced through the shaft at the transition section was obtained from Equation (24).

2.1.4 Power Transmission in the Extruder

Power was transmitted from a direct current (DC) electric motor to the speed reducer worm gear shaft with the aid of a belt drive. A multiple-grooved pulley was fitted to the speed reducer worm gear shaft. Figure 1 shows the schematic diagram of the power transmission system.

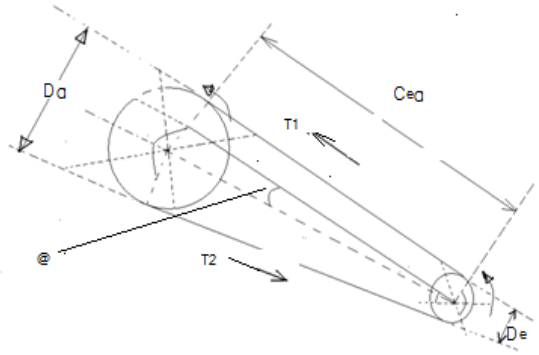

Figure 1: The Schematic Diagram of the Power Transmission System

From Figure 18, let

D_e = Diameter of the pulley fitted to the electric motor

D_a = Diameters of the multiple-grooved pulley fitted to the speed reducer worm gear shaft

T_1 and T_2 = Tension in the tight and slack side of the belt

C_{ea} = Center distance between the tho pulleys

α = Angle of lap of the smaller pulley on the big pulley

N_e = Electric motor rpm = 1440 *rpm*

N_a = Speed reducer worm gear shaft rpm

In the belt/pulley speed reduction system a small drive pulley $D_e = 80mm$ was selected so as to achive a high power transmission efficiency (smaller pulleys have a smaller contact arc). A 10 Hp / 1440 rpm DC motor was used for this design because it is readily available, meets the horsepower requirements, affordable, and small enough to comfortably fit on the extruder base.

The role of the gearbox is to reduce the motor's speed and, in turn, multiply the available torque from the motor in order to produce sufficient power to melt, mix, and pump the extrudate. With the speed reducer the motor speed is reduced to screw speed, simultaneously increasing the torque ([5] Harold et al., 2005). Typical low speed extruders employed in food processing run at about 10–40 rpm. As a result, a speed reducer is needed between the motor and the screw.

Worm gear is used mostly where the power source operates at a high speed and output is at a slow speed with high torque. Worm gears are used for transmitting torque between intersecting shafts. The shafts are normally perpendicular, though it is possible to accommodate other angles.

They are used for large speed reduction with concomitant increase in torque. Typical reduction ratios can be as low as 5:1 and as high as 40:1 ([5] Harold et al., 2005).

The driven pulley diameter was calculated from

$$N_e r_e = N_a r_a \quad \text{or} \quad N_e D_e = N_a D_a \qquad (32)$$

The maximum and minimum center distances between the two pulleys were given by (Khurmi and Gupta, 2009):

$$C_{ea_{max}} = 3(D_e + D_a) \qquad (33)$$

$$C_{ea_{min}} = 0.55(D_e + D_a) + D_a \qquad (34)$$

The center distance is given by:

$$C_{ea} = \frac{\left(C_{ea_{max}} + C_{ea_{min}}\right)}{2} \qquad (35)$$

The angle of lap of the smaller pulley on the big pulley for an open belt was given as:

$$\sin\alpha = \frac{(D_a - D_e)}{2C_{\partial}} \qquad (36)$$

From which;

$$\alpha = \sin^{-1}\left\{\frac{D_a - D_e}{2C_{ea}}\right\} \qquad (37)$$

The angle of contact of the belt on the motor pulley (θ_e) and the multiple-grooved pulley of the speed reducer gear (θ_a) were obtained as ([7] Khurmi and Gupta, 2009):

$$\theta_e = 180^0 - 2\alpha \qquad (38)$$

$$\theta_a = 180^0 + 2\alpha \qquad (39)$$

The length of the belt was obtained as follows:

$$L = \sqrt{4C_{ea}^2 - (D_a - D_e) + \frac{1}{2}(D\theta_a - D\theta_e)} \qquad (40)$$

where,

$$D\theta_a = \frac{\theta_a}{360} \times 2\pi D_a \qquad (41)$$

$$D\theta_e = \frac{\theta_e}{360} \times 2\pi D_e \qquad (42)$$

The area A of the belt can be obtained as:

$$A = wt \qquad (43)$$

The mass of the belt was given as:

m = area of belt × length of belt × density of belt material.

The mass of belt per meter length m_l was given by (Khurmi and Gupta, 2009):

$$m_l = \frac{\text{area of belt} \times \text{density of belt material}}{\text{length of belt}} \qquad (44)$$

The speed of the belt was given as:

$$v = \frac{\pi D_e N_e}{60} \qquad (45)$$

The centrifugal tension (T_c) in the belt was obtained as (Khurmi and Gupta, 2009):

$$T_c = m_l v^2 \qquad (46)$$

The maximum tension (T) in the belt can was obtained as:

$$T = \sigma A \qquad (47)$$

where, $\sigma =$ the allowable tensile stress in the belt.

The drive generates radial load. Radial load generated by a V-Belt.was given by:

$$R = \frac{9.56 \times P}{n_1} \times \frac{2000}{D} \times f \times 1.5 \qquad (48)$$

where: R = Radial Load [kN]

P = Actual Transmission Power or Motor Power [kW]

n = Input Speed [rpm]

D = High Speed Shaft Pulley Diameter [mm]

f = Compensation Factor (Given in appropriate table)

The tension in the tight side of the belt T_1 is derived as:

$$T_1 = T - T_c \qquad (49)$$

According to Hall et al., (1999), if T_2 is the tension in the slack side of the belt, then it can be derived from:

$$e^{\mu\theta_e} = \frac{T_1 - m_l v^2}{T_2 - m_l v^2} \qquad (50)$$

$$\text{i.e, } T_2 = \frac{T_1 - m_l v^2}{e^{\mu\theta_e}} + m_l v^2 \qquad (51)$$

where, $\mu =$ coefficient of friction between the belt and the groove of the pulley fitted to the electric motor.

The coefficient of friction between an oak tanned leather material and a steel pulley operating under dry condition is 0.25 (Khurmi and Gupta, 2009).

For belt transmission between the motor and the gear reducer; dimensions for standard V-belts and standard V-grooved pulley are given in appropriate Tables (IS: 2494-1974).

The power transmitted by the electric motor is given as:

$$P = (T_1 - T_2)v \qquad (52)$$

The extruder shaft forms an integral part of the machined extruder screw itself. The shaft equivalent twisting and bending moments may be evaluated from:

$$\left.\begin{aligned} T_e &= \frac{\pi}{16} \times \tau \times d^3 \\ M_e &= \frac{\pi}{32} \times \sigma_b \times d^3 \end{aligned}\right\} \qquad (53)$$

where:

τ = Shear stress induced due to twisting moment, and

σ_b = Bending stress induced due to bending moment.

For a v-belt transmitting power between 2 KW to 15 KW, the allowable tensile stress should not exceed 2MPa $(2\ \mathrm{N/mm^2})$ according to Khurmi and Gupta (2009).

2.1.5 Gear Box Rating

When a single screw extruder gearbox reduces motor speed to screw speed, it experiences generated gear forces as well as screw end pressure thrusting, and possible twisting and bending screw forces on the driveshaft. Transmitting torque by meshing of the gear teeth generates forces that act on the rotating shafts and then through the supporting bearings into the housing. The bearings, while resisting these forces, maintain the shafts in close alignment within the gearbox. The extrusion process emphasis is on power requirements, but it is the torque, or resistance to rotation, that determines the design and limitations of the gearboxes and other drive components.

Alignment of the extruder screw within the barrel begins at the gearbox when the barrel/screw shaft assembly is centered on the gearbox housing. The gearbox bearings on the output shaft provide a cantilevered support for the screw. Any bending or twisting caused by forces acting between the barrel and screws is transmitted back into the shafts and bearings. Although the gear forces themselves are constant in magnitude and direction, as long as the torque is constant, the surfaces on which they act are constantly changing because of shaft rotation. At any given point the loads are therefore cyclic and can impose fatigue type failures on critical components in the gearbox such as the gears, bearings and shafts ([5, 9] Harold etal.,2005;Timothy,2000). In selecting the type and size of the reducer, the required ratio is:

$$i_{req.} = \frac{n_1}{n_2} \qquad (54)$$

where, $n_1 =$ input speed of the reducer $\left[\min^{-1}\right]$

$n_2 =$ output speed of the reducer $\left[\min^{-1}\right]$

The corresponding nominal ratio i_N was obtained from appropriate table. To select the reducer size, the nominal power rating of the reducer was checked:

$$P_N = P_e \cdot f_1 \qquad (55)$$

where, $P_N =$ nominal reducer power

$P_e =$ effective machine power

$f_1 =$ application factor $(2.0 \le (f_1) \ge 1.5)$

The required torque,

$$T_{req.} = 9550\frac{P_N}{n_2}\cdot f_1 \qquad (56)$$

For the selection of the cooling system, the thermal limit was verified $\left(P_e \le P_t\right)$ in which (Harold et al., 2005; Timothy, 2000):

$$P_t = P_t \cdot f_w \cdot f_A \cdot f_L \qquad (57)$$

where, P_t = thermal limit power of the reducer (kW)

P_e = effective machine power

f_w = thermal factor

f_A = utilisation factor

f_L = thrust bearing factor

2.1.6 Selection of Thrust Bearing

For an approximative calculation, by neglecting possible supplementary forces of technological nature specifical to extruders, it is sufficient to suppose that: thrust Load:

$$F_{ax} = \pi \times \frac{d^2}{4\times 10000}\times P_a \qquad (58)$$

where, F_{ax} = Thrust Load/Pressure from the extruder [kN]

P_a = Working Pressure [bar or MPa]

d = Extruder Screw Diameter [mm]

The necessary dynamical bearing capacity of the thrust bearing $C_{Radial}\left[kN\right]$ is:

$$C_{req.} = f_d \cdot F_{ax} \cdot \left(\frac{L\cdot 60\cdot n}{10^6}\right)^{\frac{3}{10}} \qquad C_{req.} < C_{table.} \qquad (59)$$

where, f_d = Factor for sense of rotation (max=1.06)

F_{ax} = Thrust pressure from the extruder (kN)

L = Bearing life duration (h)

n = Speed of the extruder ($\min^{-1}$)

$C_{req.}$ = Required dynamic bearing capacity of the thrust bearing (kN)

$C_{table.}$ = Dynamic bearing capacity of the thrust bearing according to selection table (kN)

2.2 Materials of Construction

The poundo-yam extruder comprises a barrel within which a graduating screw is rotatably mounted. The extruder barrel and screw are of high strength stainless steels. The materials selected for other component parts of the poundo-yam extruder include: U- Channel and MS Angle bar (for extruder frame), speed reduction worm gear box, 10 Hp / 1440 rpm electric motor, Forged iron, 3- grooves pulley: Ø (10, 150, 200 & 250 mm dia.), thrust and radial bearings, stainless steel sheet (for extruder hopper), 10 mm thick mild steel plate (for extruder barrel bracket), B v-belt, and stainless steel bolts and nuts. Power is transmitted from the electric motor to the speed reducer worm gear shaft with the aid of a belt drive. A multiple-grooved pulley is fitted to the speed reducer worm gear shaft.

The construction of the designed extruder was carried out at the Central Workshop of School of Engineering, Federal University of Technology, Minna.

3 RESULTS

The poundo-yam extruder was designed, constructed with locally available materials and evaluated. The design concept was based on extrusion principle. A snapshot of the extruder screw full length is shown in Figure [1]. The three geometrical sections of the extruder screw are shown in Figures [2], [3], and [4]. Figures [5], [6], and [7] show the extruder main frame, the half barrel details, and the isometric view of the main assembly, respectively. The isometric view of the radial bearing housing, the main assembly details/components, and the radial bearing housing are shown in Figures [8], [9], and [10]. The orthographic projection of the assembly, the isometric view of the barrel bracket, and the assembled extruder in operation are shown in Figures [11], [12], and [13], respectively.

[8] Figure 1: Extruder Screw (Full Lenght)

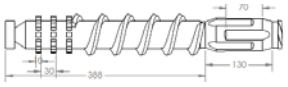

[8] Figure 2: Metering Section

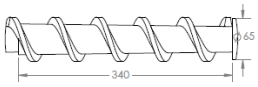

[8] Figuren 3: Feeding Section

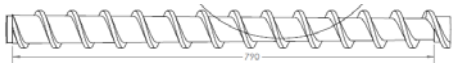

[8] Figure 4: Transition Section

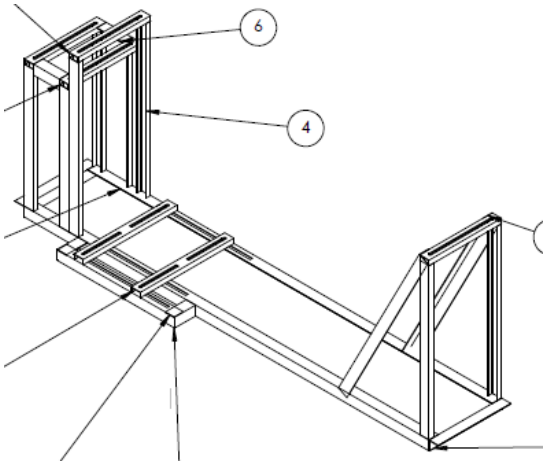

[8] Figure 5: Main Frame

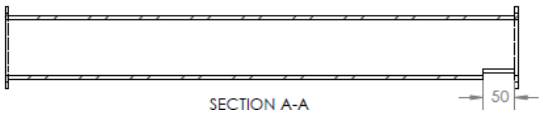

[8] Figure 6: Half Barrel Details

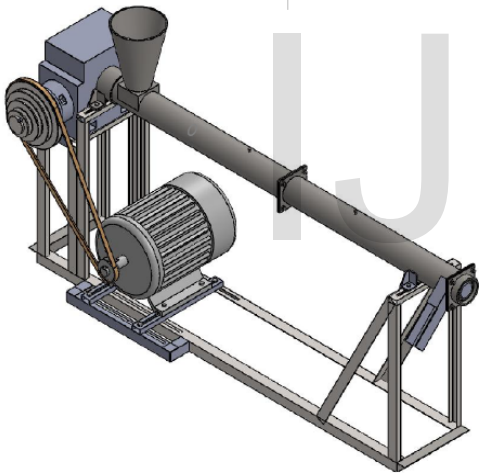

[8] Figure 7: Isometric of the Main Assembly

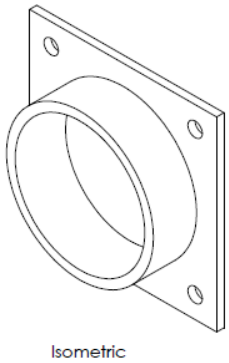

[8] Figure 8: Isometric of the Radial Bearing Housing

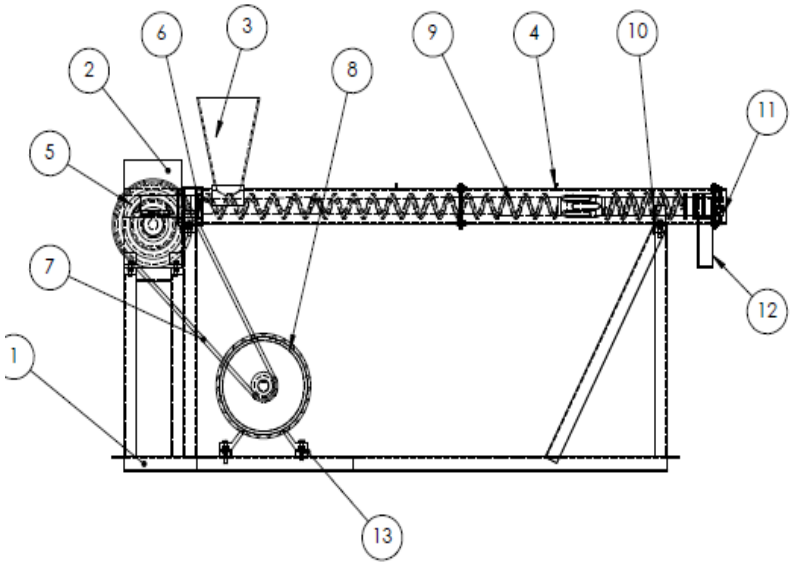

S/No	Components
1	Extruder Main Frame
2	Speed Reducer Gearbox
3	Hooper
4	Extruder Barrel
5	Multi-Grooved Pulley
6	Thrust Bearing housing
7	V- Belt
8	AC Electric motor
9	The Extruder Screw
10	Barrel Bracket
11	Radial Bearing Housing
12	Extrudate Shute/Outlet
13	Electric motor Seat

[8] Figure 9: Main Assembly Details/Components

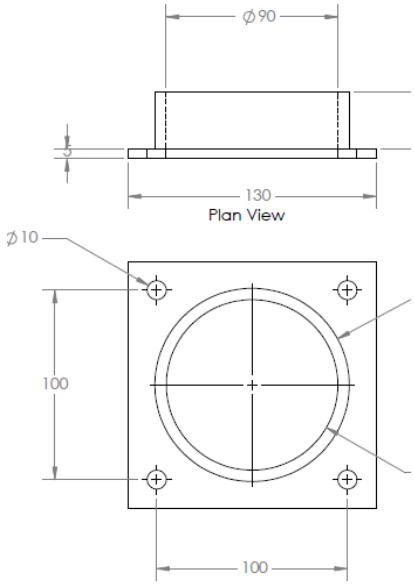

[8] Figure 10: Radial Bearing Housing

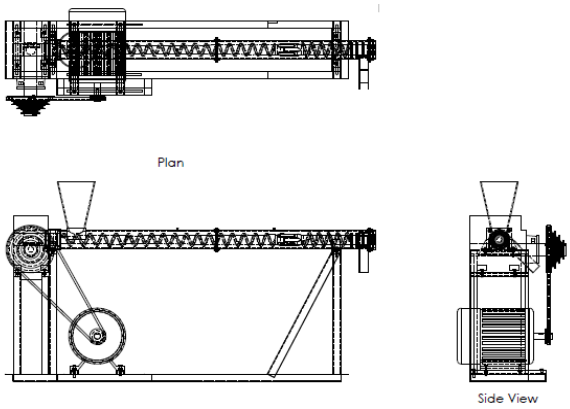

[8] Figure 11: Orthographic Projection of the Assembly

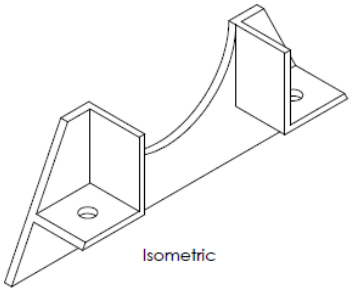

[8] Figure 12: Isometric of the Barrel Bracket

[8] Figure 13: Assembled Extruder in Operation

CONCLUSION

A poundo-yam extruder was designed, constructed and evaluated. The design concept was based on extrusion principle, and the materials of construction were locally sourced.

CONTRIBUTIONS TO KNOWLEDGE

This research work has been able to provide alternative poundo-yam equipment through the use of extrusion principles. The research work is an improvement on and/or replacement for both the current batch poundo-yam automated blender and the dominant traditional poundo-yam processing methods. The design is suitable for continuous production of poundo-yam.

REFERENCES

[1] Adjebeng-Asem. http://www.idrc.org.sg/en/ev-30793-201-1-_DO_TOPIC.html. Translating Technical Innovation into Entrepreneurship in Nigeria: Social and Policy Implications: Document(s) 15 of 29.

[2] Anil Kumar., Rakesh K. Gupta. 1997. Fundamentals of Poly mer Engineering Marcel Dekker, Inc. 270 Madison Avenue, New York, NY 10016.Pp 631-645

[3] Chang Dae Han. 2007. Rheology and Processing of Polymeric Materials Volume 2. Oxford University Press, Inc. New York. Pp. 57-58.

[4] http://www.africanfoods.co.uk/yam.html.Pounded yam

[5] Harold F. Giles , John R.Wagner and Eldridge M. Mount. (2005). Extrusion: The Definitive Processing Guide and Handbook. William Andrew, Inc., 13 Eaton Avenue, Norwich, NY 13815. Pages 13-32, 53-62, 79-81.

[6] IITA Annual Report 1997. 1998. Yams (Dioscorea).

[7] Khurmi and Gupta, 2009. A Textbook of Machine Design. S Chand & Co Ltd; 14th edition

[8] Olorunsogo, S.T. (2013): Development and Evaluation of the Performance of a Poundo-Yam Extruder. Ph.D Dissertation, Federal University of Agriculture, Abeokuta. Nigeria.

[9] Timothy W. Womer. 2000. Basic Screw Geometry. Paper pre sented at the Annual Technical Conference of the Society of Plastics Engineers Inc.

[10] Zehev Tadmor., Co s t a s g. Gog O S.2006. Principles Of Polymer Processing (2nd Edition).John Wiley & Sons, Inc., Hoboken, New Jersey. Pp.250-255, 450-474.